MIXING PROPERTIES OF SANIDINE
CRYSTALLINE SOLUTIONS:

IV. PHASE DIAGRAMS FROM EQUATIONS OF STATE[1]

D. R. Waldbaum and J. B. Thompson, Jr., *Department of Geological Sciences, Harvard University, Cambridge, Massachusetts 02138.*

Abstract

Phase diagrams involving alkali feldspars in the model system SiO_2-$NaAlO_2$-$KAlO_2$-Al_2O_3 have been calculated using a preliminary formulation of the mixing properties of sanidine crystalline solutions presented in Part III of this series. The mixing properties so obtained permit calculation of the two-feldspar coexistence surface as a function of pressure and temperature in the sub-system $NaAlSi_3O_8$-$KAlSi_3O_8$.

Provisional values of the mixing parameters for $NaAlSi_3O_8$-$KAlSi_3O_8$ liquids at one atmosphere may then be calculated from the minimum melting temperature and composition given by Schairer (1950). From these in turn we obtain preliminary estimates of the solidus for Na-rich compositions and the (metastable) solidus and liquidus in the composition range where alkali feldspar melts to leucite and a liquid displaced toward SiO_2 from the feldspar join.

The effect of the component $KAlSi_3O_8$ on equilibria between alkali feldspars, jadeite, and quartz has also been calculated tentatively for temperatures up to 1300° C and 32 kbar. The calculated four-phase equilibrium between quartz, jadeite, and two alkali feldspars intersects the line of critical solution at about 26 kbar, and terminates there at a critical end-point.

Introduction

In the preceding papers of this series (Thompson and Waldbaum, 1968, 1969; Waldbaum and Thompson, 1968) we have been concerned with the derivation of thermodynamic mixing properties of high-temperature alkali feldspars from various kinds of experimental data and have obtained therefrom some tentative analytic formulations, summarized in Part III (Thompson and Waldbaum, 1969, Table 6), for the various thermodynamic excess functions. It is our purpose here to demonstrate how such analytic formulations may be used to calculate phase diagrams of several different kinds for several different types of equilibria involving sanidine crystalline solutions and other phases. The calculated diagrams are of course based on experimental data, some of which is in the form of phase diagrams, hence we may regard the calculated diagrams below as a smoothing of pre-existing data in such a way that it must be internally consistent, and in a way that provides a reasonable extrapolation to conditions which are difficult or impractical to explore in the laboratory.

It is not at all our intention to suggest that experimental studies can

now be abandoned in favor of calculated phase diagrams, inasmuch as further empirical studies are needed to obtain improved equations of state and to test the validity of subsequent extrapolations outside the range of the original data. However, the task of studying phase equilibria in mineral systems at different temperatures and pressures can be greatly simplified by utilizing a few carefully chosen sets of experimental data rather than determining phase diagrams directly for all temperatures and pressures of possible interest. The use of an analytic formulation that obeys the constraints of an equation of state to obtain smoothed phase diagrams also assures the correct geometrical relations between stable and metastable phase boundaries. To the extent that such a formulation approximates the true equation of state, it provides a quantitative basis for evaluating a mineral assemblage as an equilibrium (whether it be partial or complete equilibrium) or non-equilibrium assemblage under a given set of conditions.

The calculations below are based on a tentative formulation of the excess thermodynamic properties of sanidine crystalline solutions as obtained in Part III from two-phase data for high-temperature alkali feldspars synthesized from peralkaline starting materials. As discussed in Part III (p. 000), from comparison with data from exchange experiments, the excess Gibbs energy of mixing for high-temperature, monoclinic alkali feldspars is probably somewhat greater than is indicated by the formulation based only on two-phase data. Although other formulations would serve as well for the illustrative calculations and diagrams below, the one selected has the advantage of simplicity, and is consistent with the data of greatest geologic interest.

We shall then write for the molar excess Gibbs energy:[2]

$$\overline{G}_{\text{ex}}(P, T) = (6326.7 + 0.0925P - 4.6321T)N_1N_2^2 \\ + (7671.8 + 0.1121P - 3.8565T)N_2N_1^2 \tag{1}$$

where T is temperature (°K), P denotes pressure (bars) and N_1 and N_2 are the mole fractions of the components $NaAlSi_3O_8$ and $KAlSi_3O_8$, respectively. The numerical coefficients (Margules parameters) are based on data ranging from 500 to 700°C and from 2 to 10 kbar. Computations within this temperature and pressure range are subject to the restriction that the Margules parameters are no more reliable than the data used to obtain them, and are essentially a partly statistical and partly interpretative smoothing of these data (see detailed discussion in Part III).

---

[2] Enough significant figures in the coefficients are given in order to avoid roundoff error in computations, and their number is in no way an index of the precision or accuracy of the values (see Part III).

Computations outside this range must thus be regarded as a consistent extrapolation of these data, and of our interpretation of them. The numerical values in (1) are likely to change as new data are obtained (internal Al-Si ordering, for example, is not yet taken into account), but the results given here must be qualitatively like the correct ones and quantitatively not far off the mark.

Equation (1), as discussed in Part III of this series, has values selected (within the uncertainty of the data and its interpretation) so that the critical phases lie on a straight line in P-T-N space, and have a constant composition. For this special case all isobaric sections of the calculated binodal and spinodal surfaces are identical in terms of T/T_c and N (Table 1, and Figure 13 of Part III).

Even if the values of the coefficients in (1) and (2) could be regarded as substantially correct for sanidine, the equilibria calculated below must in part be metastable with respect to equilibria involving triclinic feldspars or monoclinic feldspars with a higher degree of ordering between the T_1 and T_2 tetrahedral sites than is found in sanidine (see Thompson, 1969, p. 352–363).

Mixing Properties

The molar internal energy ($\overline{E}$), volume ($\overline{V}$), and entropy ($\overline{S}$) of mixing of sanidine solutions as implied by (1) are

$$\overline{E}_{\mathrm{mix}} = \overline{E}_{\mathrm{ex}} = 6326.7 N_1 N_2^2 + 7671.8 N_2 N_1^2 \text{ cal mole}^{-1} \tag{2a}$$

$$\overline{V}_{\mathrm{mix}} = \overline{V}_{\mathrm{ex}} = 0.0925 N_1 N_2^2 + 0.1121 N_2 N_1^2 \text{ cal bar}^{-1} \text{ mole}^{-1} \tag{2b}$$

$$\overline{S}_{\mathrm{mix}} = \overline{S}_{\mathrm{ex}} + \overline{S}_{\mathrm{ideal}} = 4.6321 N_1 N_2^2 + 3.8565 N_2 N_1^2$$
$$- R(N_1 \ln N_1 + N_2 \ln N_2) \text{ cal deg}^{-1} \text{ mole}^{-1} \tag{2c}$$

$$\overline{S}_{\mathrm{ideal}} = - R(N_1 \ln N_1 + N_2 \ln N_2) \text{ cal deg}^{-1} \text{ mole}^{-1} \tag{2d}$$

where R is the gas constant (1.98726 cal deg^{-1} mole^{-1}). Mixing properties calculated from (2a, b, c) are plotted in Figure 1 for 650°C and 10 kbar as light solid lines. The entropy of mixing at the equimolar composition given by (2c) is approximately twice that for an ideal solution (dashed line). The summation of these three mixing properties, as given by (1) is shown as a heavy solid line, which has regions of both positive and negative curvature indicating that a two-phase region must be present in the phase diagram at this temperature and pressure. The points of double-tangency to the curve (binodal points) are at $N_2 = 0.0856$ and $N_2 = 0.7104$, and the points of inflection (spinodal points) are at $N_2 = 0.1773$ and $N_2 = 0.5571$. Although the excess functions given by (2) do not appear to be markedly asymmetric, their sum in Figure 1 leads to a
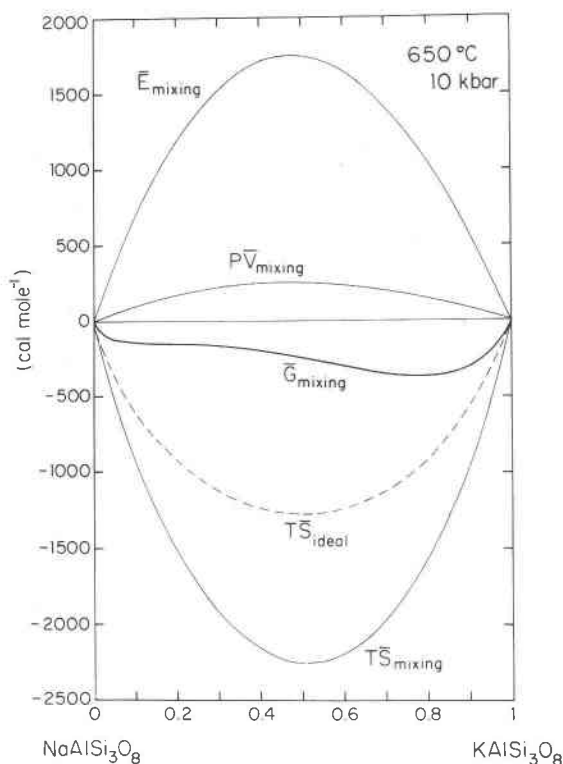
Fig. 1. Mixing properties of sanidine solutions at 650°C and 10 kbar. Heavy solid line indicates summation of $P\overline{V}_{ex}$, $T(\overline{S}_{ideal}+\overline{S}_{ex})$, and $\overline{E}_{ex}$. Dashed line represents $T\overline{S}_{ideal}$. Reference state is mechanical mixture of pure end-member phases at 650°C and 10 kbar.

highly asymmetric curve in $\overline{G}_{mix}$. The asymmetry in the excess properties is better illustrated by the trace of the rectilinear diameter (r.d.), that is, the mean composition of the coexisting phases as shown in Figure 2; and in the relative activities of $NaAlSi_3O_8$ and $KAlSi_3O_8$ as plotted in Figure 3.

It is apparent from Figure 1 that the contribution of the excess volume of mixing to the Gibbs energy is not negligible, as suggested by Perchuk and Ryabchikov (1968, p. 137–138)[1]. The $\overline{V}_{ex}$ of (2b), furthermore, though based on Part III calculations, must be quantitatively nearly correct inasmuch as it is consistent, within the limits of uncertainty, with the direct volume data discussed in Part II. Comparisons of Figures 1 and 2 also indicates the effect of pressure on phase equilibria of alkali feldspars. At 10 kbar and 650°C the difference in composition of the coexisting
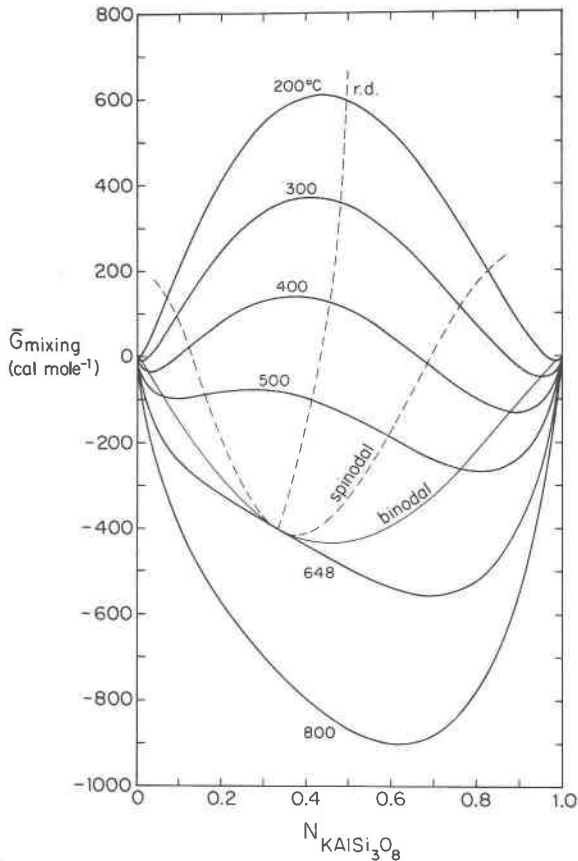
See note added in proof.

Fig. 2. Isobaric-polythermal projection of Gibbs energy of mixing surface of sanidine solutions at 1 bar. Trace of binodal curve on the surface is shown by a light solid line. Spinodal curve (dashed line) passes through points of inflection on the isothermal sections of the surface. All compositions between binodal and spinodal curves are metastable with respect to diffusion. Reference state is mechanical mixture of pure end-member phases at the stated temperature and 1 bar.

feldspars is 62.5 mole percent, whereas at 650°C and 1 bar, no two-phase region exists.

The effect of pressure on the two-phase region is summarized by the following equations

$$T_c(°K) = 921.23 + 13.4607 P_c(\text{kbar}) \tag{3a}$$

$$N_{2c} = \tfrac{1}{3} \tag{3b}$$

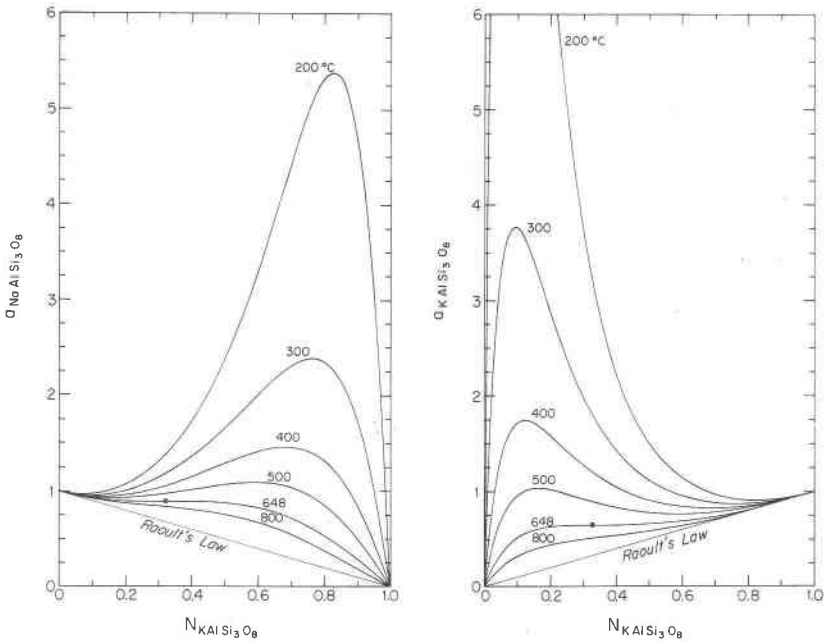Combining (3a) with the values in Table 1 leads to binodal and spi-

FIG. 3. Activities of (a) NaAlSi$_3$O$_8$ and (b) KAlSi$_3$O$_8$ in sanidine crystalline solutions at 1 bar. Reference states are the pure end-member phases at the stated temperature and 1 bar. Solid circles denote critical point.

nodal curves at any given pressure. It should be borne in mind when using Table 1 to calculate the compositions of coexisting phases that the results can be approximately correct only for highly disordered monoclinic alkali feldspars (as emphasized in Parts I and III). Goldsmith and Laves (1961) and more recently Bachinski and Orville (1968, and Bachinski, 1968, written communication) have shown that the critical temperature of highly Al-Si-*ordered*, triclinic feldspars (at 1 atm) may be as much as 200°C higher than that for sanidine. The compositions of internally equilibrated coexisting feldspars are likely, therefore, to be different from those given in Table 1 for the lower temperatures of geologic interest.

CHEMICAL POTENTIALS

The chemical potentials may be written

$$\mu_1 = \overline{G} - N_2 \left(\frac{\partial \overline{G}}{\partial N_2} \right)_{P,T} \tag{4a}$$

$$\mu_2 = \overline{G} + N_1 \left(\frac{\partial \overline{G}}{\partial N_2} \right)_{P,T} \tag{4b}$$

where

$$\overline{G} = N_1\mu_1^\circ(P, T) + N_2\mu_2^\circ(P, T) + RT(N_1 \ln N_1 + N_2 \ln N_2) + \overline{G}_{ex}(P, T) \qquad (5)$$

and the superscript $^\circ$ indicates a property of a pure end-member phase at the temperature and pressure under consideration. Equilibrium relations among the chemical potentials are shown quantitatively in Figure 4 at 500°C and 1 bar using the elements in their standard states as a reference state (Robie and Waldbaum, 1968), where:

$$\mu_1^\circ = \overline{G}_{f,773(\text{high-albite})}^\circ = -799{,}578 \text{ cal mole}^{-1}$$
$$\mu_2^\circ = \overline{G}_{f,773(\text{sanidine})}^\circ = -808{,}440 \text{ cal mole}^{-1}$$

At complete equilibrium between phases α and β, we must have

$$\mu_{1\alpha} = \mu_{1\beta} \qquad (6a)$$
$$\mu_{2\alpha} = \mu_{2\beta} \qquad (6b)$$

The compositions of α and β are connected by the horizontal solid lines in Figure 4a.

Figure 4 illustrates the relations among the chemical potentials derived from (1) for two-phase exchange equilibria as discussed in Part I. The condition for such an exchange chemical equilibrium (a *partial* equilibrium) is that

$$\left[\left(\frac{\partial \overline{G}}{\partial N_2}\right)_{\alpha'}\right]_{P,T} = \left[\left(\frac{\partial \overline{G}}{\partial N_2}\right)_{\beta'}\right]_{P,T} = (\mu_2 - \mu_1)_{\alpha'} = (\mu_2 - \mu_1)_{\beta'} \qquad (7)$$

where α' and β' denote phases in exchange equilibrium with each other. The compositions of two such phases are shown in Figure 4b connected by a horizontal dashed line. In fact, any horizontal line connecting the compositions of phases having the same value of $(\mu_2 - \mu_1)$ satisfies (7), but the conditions for complete equilibrium (6) are only met by the two compositions connected by the solid horizontal lines in Figures 4a and 4b. That (6) is not in general satisfied by compositions that coexist *only* in exchange equilibrium is shown clearly by the horizontal dashed lines in Figure 4a which correspond to the single horizontal dashed line in Figure 4b.

Figure 4b also illustrates another relationship among the chemical potentials that is satisfied only for coexisting phases in complete equilibrium. We have

$$\overline{G}_\beta - \overline{G}_\alpha = (\mu_2 N_{2\beta} + \mu_1 N_{1\beta}) - (\mu_2 N_{2\alpha} + \mu_1 N_{1\alpha})$$
$$= (N_{2\beta} - N_{2\alpha})(\mu_2 - \mu_1) \qquad (8)$$

which may also be written, for a constant temperature and pressure, as

$$\overline{G}_\beta - \overline{G}_\alpha = \int_{N_2=N_{2\alpha}}^{N_2=N_{2\beta}} \left(\frac{\partial \overline{G}}{\partial N_2}\right)_{P,T} dN_2 \qquad (9a)$$

or as

$$\overline{G}_\beta - \overline{G}_\alpha = \int_{N_2=N_{2\alpha}}^{N_2=N_{2\beta}} (\mu_2 - \mu_1) dN_2 \qquad (9b)$$

The area between the horizontal line rv and the abscissa is given by (8). Similarly, from (9), the area between $rstuv$ and the abscissa must also equal $(\overline{G}_\beta - \overline{G}_\alpha)$, hence

$$\oint_{rstuvtr} (\mu_2 - \mu_1)_{P,T} dN_2 = 0 \qquad (10)$$

and the two shaded areas in Figure 4b must be equal.

TABLE 1. CALCULATED BINODAL AND SPINODAL POINTS IN THE SYSTEM
NaAlSi$_3$O$_8$-KAlSi$_3$O$_8$ AT 1 ATM. THESE VALUES ALSO APPLY AT HIGHER
PRESSURES FOR THE SAME VALUES OF T/T_c (T IN °K)

T/T_c	Binodal		Spinodal	
	$N_{2\alpha}$	$N_{2\beta}$	$N_{2\alpha}$	$N_{2\beta}$
1.0000	0.3333	0.3333	0.3333	0.3333
0.9999	.324	.343	.328	.339
.999	.305	.363	.317	.350
.995	.272	.400	.298	.372
.990	.248	.430	.283	.389
.98	.216	.472	.264	.413
.97	.193	.506	.250	.433
.96	.174	.535	.238	.450
.95	.159	.562	.228	.465
.94	.145	.585	.220	.480
.93	.134	.608	.212	.493
.92	.123	.628	.204	.506
.90	.105	.667	.192	.529
.88	.090	.701	.180	.551
.86	.077	.733	.170	.572
.84	.065	.762	.161	.591
.82	.056	.789	.153	.610
.80	.048	.813	.145	.628
.78	.040	.836	.138	.645
.75	.031	.866	.128	.670
.70	.020	.908	.113	.709
.65	.012	.940	.010	.775
.60	.0068	.9630	.088	.778
.55	.0035	.9790	.077	.808
.50	.0016	.9891	.068	.836

Digital computer procedures have been developed (Waldbaum, 1966) which make use
of the equal-area relation to solve for the compositions of coexisting phases of a solution
whose excess functions have an analytic expression such as (1). The equal-area method is a
considerable improvement over the graphical method used to obtain the points of double-
tangency on the Gibbs surface in that coexisting compositions can be obtained accurately
even in a region of near-zero curvature ($T \approx T_{\text{critical}}$). However, this method is not readily
adapted to the restricted memory allocations of many time-shared computers and is
economical only if a high-speed machine such as an IBM 7094 is available. We have found,
moreover, that (6a) and (6b) can be solved directly for $N_{2\alpha}$ and $N_{2\beta}$ much more rapidly
and efficiently (even on a relatively small and slow computer) by iterative methods. An
iterative procedure written in a JOSS-type interpretive language such as CAL (Scientific
Data Systems, Inc.) requires only 6 statements compared with approximately 110 arith-
metic and logical statements in FORTRAN for the equal-area method. Under some circum-
stances iterative solutions to equations containing transcendental terms may diverge or
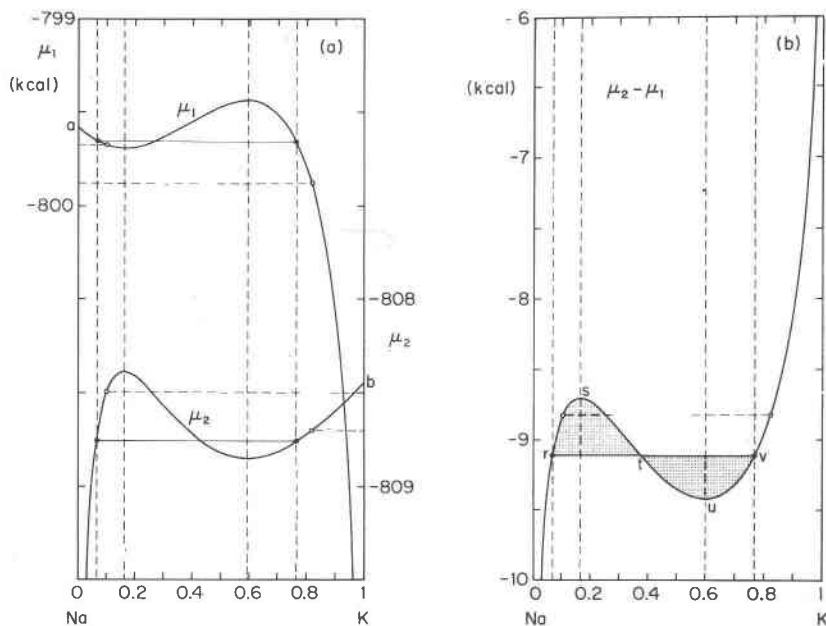may yield physically impossible results unless the initial trial parameters and subsequent

FIG. 4. a) Chemical potentials of $KAlSi_3O_8$ and $NaAlSi_3O_8$ at 500°C and 1 bar referred to the elements in their standard states at the same temperature and pressure. b) Alkali *exchange potential*, $\mu_K - \mu_{Na}(=\mu_2 - \mu_1)$, for the same P and T. Binodal and spinodal compositions are shown by dashed vertical lines. Value of μ_2 at point b denotes $\mu_2°$; value of μ_1 at a denotes $\mu_1°$.

residuals of iteration are closely controlled during the iteration cycle (this is also especially true in solving equations 12a and 12b). For this reason, it is advisable to use the equal-area method if interactive computer facilities are not available. Other useful graphical and numerical methods for solving for the compositions of coexisting phases have been discussed by Seltz (1935), Scatchard (1940), and Hala, Pick, Fried, and Vilim (1967). Seltz's (1935) method for crystal-liquid or liquid-vapor equilibria would appear to be readily adaptable to solution by digital computer.

MELTING RELATIONS AT ONE ATMOSPHERE

Treatment of experimental data. The conditions for equilibrium between a feldspar (F) and a liquid (L) in this binary system at constant temperature and pressure are

$$\Delta\mu_1 = \mu_{1L} - \mu_{1F} = 0 \tag{11a}$$

$$\Delta\mu_2 = \mu_{2L} - \mu_{2F} = 0 \tag{11b}$$

Thus,

$$N_{2L}^2[W_{G1L}+2(W_{G2L}-W_{G1L})N_{1L}]-N_{2F}^2[W_{G1F}+2(W_{G2F}-W_{G1F})N_{1F}]$$

$$=RT\ln\frac{N_{1F}}{N_{1L}}-\Delta\mu_1^{\,\circ}\quad(12a)$$

$$N_{1L}^2[W_{G2L}+2(W_{G1L}-W_{G2L})N_{2L}]-N_{1F}^2[W_{G2F}+2(W_{G1F}-W_{G2F})N_{2F}]$$

$$=RT\ln\frac{N_{2F}}{N_{2L}}-\Delta\mu_2^{\,\circ}\quad(12b)$$

It is necessary here to have as auxiliary data the quantities $\Delta\mu_1^{\,\circ}$ and $\Delta\mu_2^{\,\circ}$ and the mixing parameters of the crystalline solutions as functions of temperature. The quantities $\Delta\mu_1^{\,\circ}$ and $\Delta\mu_2^{\,\circ}$ used in these calculations were
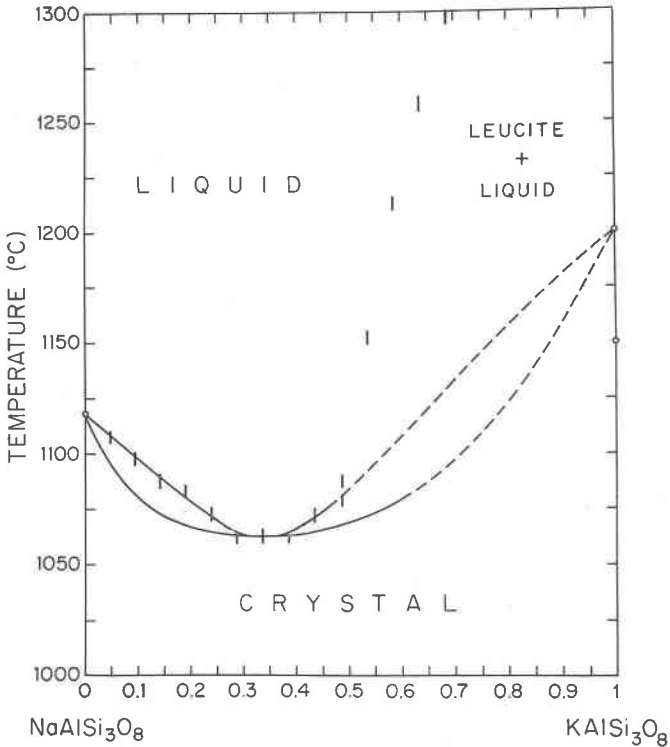

FIG. 5. Solidus and liquidus in the system $NaAlSi_3O_8$-$KAlSi_3O_8$ at 1 atm. Solid lines denote stable phase boundaries; dashed lines denote phase boundaries metastable with respect to leucite and SiO_2-rich liquids in the system SiO_2-$NaAlO_2$-$KAlO_2$ Circles denote congruent melting temperatures of high-albite and sanidine (Waldbaum, 1968) and the incongruent melting temperature of sanidine (1150°C; Schairer, 1950). Vertical bars represent Schairer's (1950) liquidus data.

obtained from the high-temperature data of Robie and Waldbaum (1968) for high-albite and sanidine, and the mixing parameters of the crystals are given by (1). The melting temperature of high-albite is reasonably well established at 1118°C. The metastable congruent melting temperature of sanidine was estimated by Waldbaum (1968) to be 1200 ± 40°C. Both temperatures are internally consistent with the data of Robie and Waldbaum.

The principal data used in these calculations are the results of Schairer (1950) for the $NaAlSi_3O_8$-$KAlSi_3O_8$ liquidus. Schairer's results are shown in Figure 5 as vertical bars indicating the temperature intervals that bracket the liquidus. Unfortunately no data exist for the compositions of the crystals coexisting with these liquids, except at the end members and at the minimum, where the crystal and liquid must have identical compositions. Therefore, only the minimum itself yields sufficient data to apply equations (12). Schairer's (1950) data give a minimum temperature of 1062.5 ± 3°C and a minimum composition of 33.66 ± 3.0 mole percent $KAlSi_3O_8$.

Margules parameters of $(Na,K)AlSi_3O_8$ *liquids.* At the minimum $N_{2L} = N_{2F}$, hence to obtain the Margules parameters of the liquid

$$W_{G1L} = \frac{1}{D} \left[A(N_1^2 - 2N_2N_1^2) - 2BN_1N_2^2 \right] \tag{13a}$$

$$W_{G2L} = \frac{1}{D} \left[B(N_2^2 - 2N_1N_2^2) - 2AN_2N_1^2 \right] \tag{13b}$$

where

$$A \equiv \left[W_{G1F} + 2(W_{G2F} - W_{G1F})N_1 \right] N_2^2 - \Delta\mu_1^\circ$$
$$B \equiv \left[W_{G2F} + 2(W_{G1F} - W_{G2F})N_2 \right] N_1^2 - \Delta\mu_2^\circ$$
$$D \equiv (N_2^2 - 2N_1N_2^2)(N_1^2 - 2N_2N_1^2) - 4(N_1N_2)^3$$

Using Schairer's (1950) value of the minimum composition ($N_2 = 0.3366$), we obtain the following values for the liquid phase at 1335.65°K

$$\left. \begin{aligned} W_{G1L} &= -\ 2436 \text{ cal mole}^{-1} \\ W_{G2L} &= -\ 1713 \text{ cal mole}^{-1} \end{aligned} \right\} \tag{14}$$

from which the Gibbs energy of mixing of the liquid may be calculated (Fig. 6b).

Such liquids are not truly binary solutions (they are actually quaternary), but the agreement between the observed and calculated liquidus
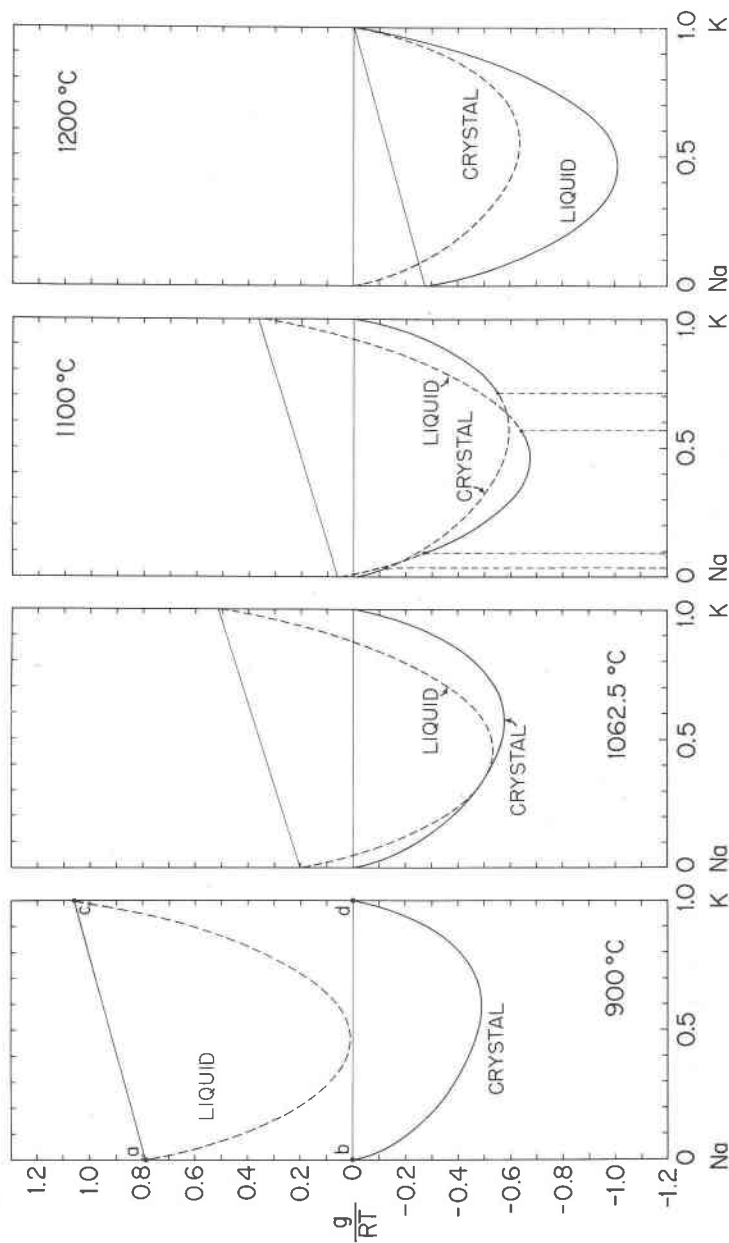
FIGURE 6. Gibbs energies of mixing of crystalline and liquid (Na,K)AlSi$_3$O$_8$ solutions referred to a mechanical mixture of end-member crystalline phases at 1 atm,

$$g \equiv \overline{G}(\text{crystal or liquid}) - N_1 \mu_1^{\circ}{}_{,\text{crystal}} - N_2 \mu_2^{\circ}{}_{,\text{crystal}}$$

Dashed curves denote metastable compositions; heavy solid curves denote stable compositions. (a) 900°; (b) 1062.5°; (c) 1100°; (d) 1200°C.

in Figure 5 (discussed below) suggests that the simple approach used here is not unreasonable for liquids in which the only permitted compositional variation is in the ratio of Na to K.

Inasmuch as crystal-liquid equilibrium data for only one temperature are used to obtain (14), it is not possible to obtain a polythermal equation of state for the liquids. Hence it is necessary to assume either that the excess entropies *or* the excess enthalpies of mixing in the liquid are zero in order to use the present results at other temperatures. For reasons discussed below we have assumed that the excess entropies of mixing are zero, thus

$$\left.\begin{array}{l} W_{H1L} = W_{G1L} = -2436 \text{ cal mole}^{-1} \\ W_{H2L} = W_{G2L} = -1713 \text{ cal mole}^{-1} \end{array}\right\} \qquad (15)$$

Calculated phase diagram. With the mixing properties of both crystal and liquid expressed in tentative numerical form it is now possible to compute the Gibbs energies of mixing of both phases as a function of temperature. Figure 6 shows the results of calculations for 900, 1062.5, 1100, and 1200°C. The compositions of phases coexisting in equilibrium at 1100°C, shown by vertical dashed lines in Figure 6c, are 3.5 and 71.1 mole percent for the solidus, and 9.0 and 56.8 percent for the liquidus. Schairer's (1950) data indicated that for a bulk composition of 9.5 percent, the liquidus is between 1095 and 1100°C. No comparable data exist on the K-rich side of the minimum since above 1080°C K-rich feldspars melt incongruently to two-phase mixtures containing leucite and a liquid displaced toward SiO_2 from the feldspar join.

The solidus and liquidus may be computed directly from (12), but it is necessary to use iterative methods because of the transcendental and cubic terms in the equations. The results obtained by solving for N_{2L} and N_{2F} at a given temperature are summarized in Table 2 and in Figure 5. The liquidus is in good agreement with the remainder of Schairer's data; the solidus is also reasonable, but there are no available data with which to compare it.

Similar computations were carried out by assuming the enthalpy of mixing to be zero, and that the excess Gibbs energy is due entirely to the excess entropy of mixing. The excess Gibbs energy of the liquids is, in fact, probably some combination of both, but the assumption of zero excess entropy yields a liquidus which is in better agreement with that of Schairer.

The above assumption can be tested in a number of ways—the most obvious being a determination of the compositions of feldspars coexisting with liquids in experiments such as Schairer's (1950). This would permit study of the temperature variation of the excess parameters over a

TABLE 2. CALCULATED SOLIDUS AND LIQUIDUS IN THE SYSTEM NaAlSi$_3$O$_8$-KAlSi$_3$O$_8$ AT 1 ATM. BOTH SOLIDUS AND LIQUIDUS ON THE K-SIDE OF THE MINIMUM ARE METASTABLE WITH RESPECT TO LEUCITE AND A SILICA-RICH LIQUID ABOVE 1080°C (SCHAIRER, 1950).

$T(°C)$	Liquidus		Solidus	
	N_{2L}	N_{2L}	N_{2F}	N_{2F}
1200	0.000	—	0.000	—
1190	.947	—	.978	—
1180	.898	—	.954	—
1170	.853	—	.930	—
1160	.810	—	.904	—
1150	.768	—	.877	—
1140	.727	—	.849	—
1130	.687	—	.819	—
1120	.648	—	.787	—
1110	.608	0.041	.751	0.014
1100	.568	.090	.711	.035
1090	.526	.139	.664	.062
1085	.504	.164	.634	.080
1080	.490	.190	.604	.101
1075	.455	.217	.567	.129
1070	.426	.248	.518	.167
1065	.386	.287	.444	.232
1063	.358	.315	.385	.288
1062.5	.3366	.3366	.3366	.3366

temperature interval of only 70°, but the fact that liquids of feldspar composition are able to persist as glasses for long periods of time, even at high temperatures, suggests that metastable exchange equilibria in this system might be studied to advantage at lower temperatures. Goldsmith and Laves (1961) have shown, in fact, that mixtures of crystalline feldspars and glasses exchange alkalis readily between 800 and 1000°C. It should be possible, therefore, to make use of the exchange equilibrium relations in (7) to determine Margules parameters of the liquids. (The phases α' and β' may be thought of here as crystal and liquid, respectively.) This can be visualized graphically in Figure 6a by drawing parallel tangents to the two curves (Part I, Fig. 1a). The compositions corresponding to pairs of parallel tangents at 900°C are shown in Figure 7 (which shows the close analogy to a simple ternary reciprocal exchange system; see also Mueller, 1964). Experimental studies of this type can probably be extended to 500 or 600°C where the alkali diffusion rates are still large enough to achieve equilibrium within a reasonable
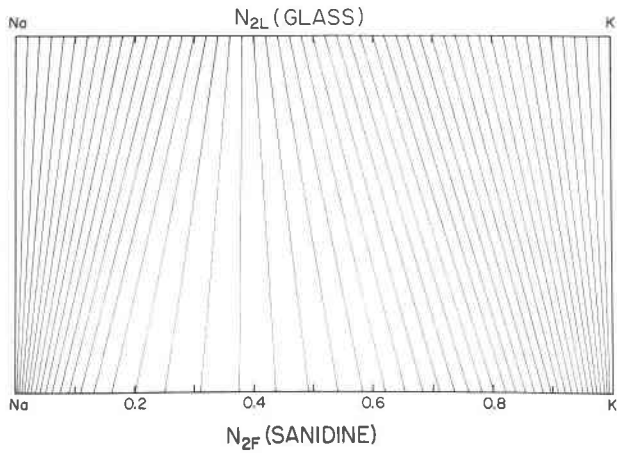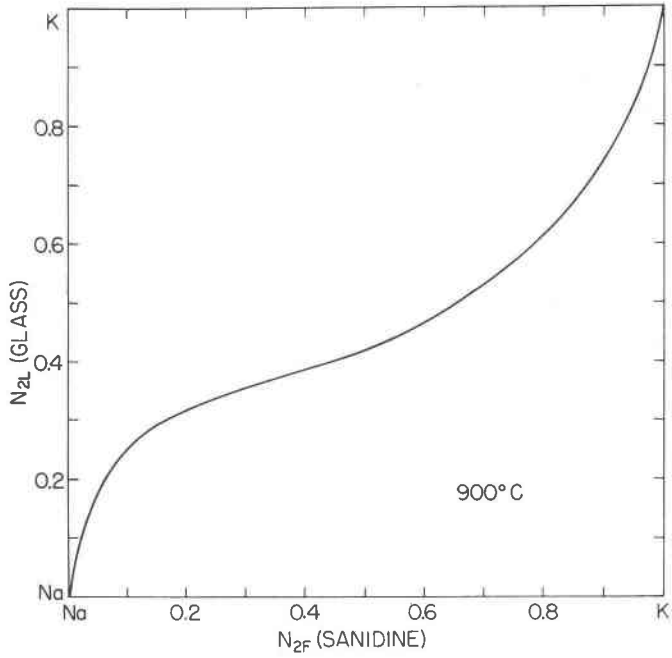
FIG. 7. Calculated ion-exchange (Na−K) equilibrium relations between (Na, K)AlSi$_3$O$_8$ crystalline and glass solutions at 900°C and 1 atm.

period of time, and thus yield a substantially greater temperature interval for determining W_{HL} and W_{SL}.

FELDSPAR-JADEITE-QUARTZ EQUILIBRIA

The calculations above can be extended to systems of more components provided the equations of state of the other phases are known, and the feldspars are such that they can be represented adequately by (1). A simple extension is to the system $NaAlO_2$-$KAlO_2$-SiO_2 which includes such additional phases as quartz, coesite, jadeite, nepheline, and leucite. Although phase equilibria in the binary system SiO_2-$NaAlO_2$ have been the subject of numerous experimental studies (Kracek, Neuvonen, and Burley, 1951; Robertson, Birch, and MacDonald, 1957; Birch and LeComte, 1960; Bell, 1964; Hlabse and Kleppa, 1968; Boettcher and Wyllie, 1968; and Newton and Kennedy, 1968), the effect of the $KAlSi_3O_8$ component on the equilibria between alkali feldspars, jadeite, and quartz has not yet been investigated in detail. Sufficient thermodynamic data are now at hand, however, to make preliminary calculations of these equilibria.

Thermodynamic relations. The equilibrium condition at constant temperature and pressure for the assemblage *quartz-alkali feldspar-jadeite* may be obtained by considering the following stoichiometric relation among the components of the phases

$$NaAlSi_3O_8 - SiO_2 - NaAlSi_2O_6 = 0 \qquad (16)$$

hence let us define

$$\Delta\mu_1 \equiv \mu_{NaAlSi_3O_8, F} - \mu_{SiO_2, Q} - \mu_{NaAlSi_2O_6, J} \qquad (17)$$

which must be zero at equilibrium. Let

$$\Delta\mu_1^{\circ} \equiv \mu_{1F}^{\circ} - \mu_{SiO_2, Q}^{\circ} - \mu_{NaAlSi_2O_6, J}^{\circ} \qquad (18)$$

We also have

$$\mu_{1F, mix} = \mu_{1F} - \mu_{1F}^{\circ} \qquad (19a)$$

$$= RT \ln N_1 + W_{G1} N_2^2 + 2(W_{G2} - W_{G1}) N_1 N_2^2 \qquad (19b)$$

where the subscripts 1 and 2 denote the feldspar components, as above; F is feldspar, Q is quartz, and J is jadeite. Combining (17), (18), and (19a), and because quartz and jadeite are pure substances in this system, we have

$$\Delta\mu_1 = \Delta\mu_1^{\circ} + \mu_{1F, mix} = 0 \qquad (17a)$$
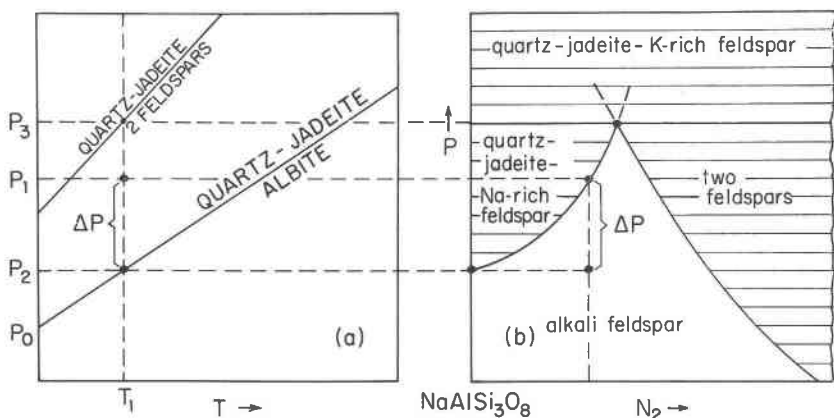
Fig. 8. (a) Pressure-temperature relations for *quartz-alkali feldspar-jadeite* equilibria. (b) Pressure-composition relations at $T = T_1$. Compare Robertson, Birch, and MacDonald (1957, p. 134). Equilibria shown are isothermal and for bulk compositions along the line $NaAlSi_3O_8$-$KAlSi_3O_8$. Two-phase *quartz-jadeite* tie-lines appear as points along the $NaAlSi_3O_8$ edge of the diagram.

When the feldspar is pure $NaAlSi_3O_8$ we have

$$\Delta\mu_1 = \Delta\mu_1^{\circ} = 0 \qquad (17b)$$

as the equilibrium condition along the curve for the simpler system SiO_2-$NaAlO_2$ as determined by Birch and LeComte (1960) and others.

Let us now consider the variation of the chemical potential of $NaAlSi_3O_8$ in sanidines with composition at a given pressure, P_1, and temperature, T_1, at which quartz, jadeite, and alkali feldspar are in equilibrium. For any feldspar outside the two-feldspar field, other than one that is pure $NaAlSi_3O_8$, we must have $\mu_1 < \mu_1^{\circ}$, hence $\mu_{1F,mix} < 0$ (Fig. 4a). Hence from (17a) it follows that

$$\Delta\mu_1^{\circ} > 0 \qquad (20)$$

for such alkali feldspars in equilibrium with jadeite and quartz. Since $\Delta\bar{S}_1^{\circ} > 0$, T_1 must be less than the temperature of the *quartz-albite-jadeite* curve for the K-free system at P_1 (Fig. 8a) in order to satisfy (20). This is also illustrated in Figure 9d for potassium-rich feldspars in equilibrium with jadeite and quartz, and in Figure 9c where the feldspar in equilibrium with jadeite and quartz is nearly pure albite. Similarly, since $\Delta\bar{V}_1^{\circ} > 0$, P_1 must be greater than the pressure P_2 of the curve for the K-free system at T_1, as shown schematically in Figures 8a and 8b.

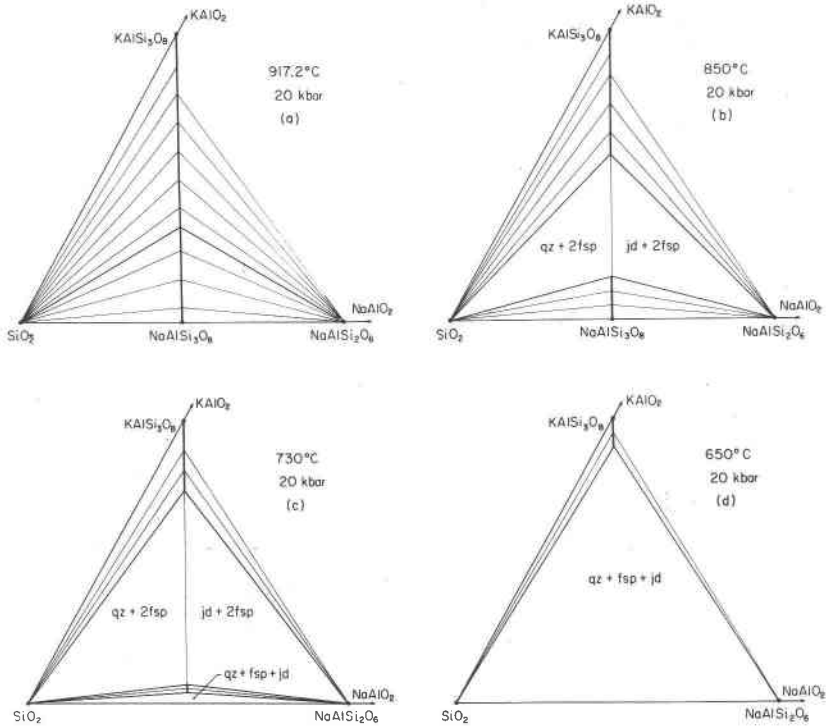Therefore, to determine points on the *quartz-alkali feldspar-jadeite*

FIG. 9. Calculated isothermal-isobaric composition phase relations in the silica-rich portion of the system SiO_2-$NaAlO_2$-$KAlO_2$ at 20 kbar. Pure albite is in equilibrium with jadeite and quartz at 738°C at this pressure.

equilibrium in P-T-N_{2F} space, we may compute the effect of pressure on $\Delta\mu_1^\circ$, at T_1, from

$$\int_{P_2}^{P_1} d\Delta\mu_1^\circ = \int_{P_2}^{P_1} \Delta\overline{V}_1^\circ dP \tag{21}$$

Neglecting the thermal expansions and compressibilities of the phases we may regard $\Delta\overline{V}_1^\circ$ as constant and not significantly different from its value at 1 atmosphere and 298.15°K. Noting from (17b) that $\Delta\mu_1^\circ$ at P_2 and T_1 must be zero, we have at P_1 and T_1,

$$\Delta\mu_1^\circ = \Delta\overline{V}_1^\circ(P_1 - P_2) \tag{22}$$

The equilibrium condition may then be written

$$\mu_{1F,mix} + \Delta\overline{V}_1^\circ(P_1 - P_2) = 0 \tag{17c}$$

which may be solved directly for P, T, or N_{2F} given any two of the variables.

In the computations that follow, T was selected as the dependent variable. Recalling that

$$W_G = W_E + PW_V - TW_S \tag{23}$$

and assuming that the equilibrium curve for the K-free system is linear in P-T coordinates above 400°C (although this should not be strictly true when the effects of compressibility, thermal expansion, heat capacity, and Al–Si ordering are taken in account), we may then write

$$P_2 = P_0 + T_1(dP/dT)^\circ_{QAJ} \tag{24}$$

where P_0 is the (extrapolated) equilibrium pressure at absolute zero. Combining (17c), (19b), (23), and (24), we obtain

$$T_1 = \frac{N_2^2\{2N_1[W_{E1} - W_{E2} + P_1(W_{V1} - W_{V2})] - (W_{E1} + P_1W_{V1})\} - (P_1 - P_0)\Delta\bar{V}_1^\circ}{N_2^2[2N_1(W_{S1} - W_{S2}) - W_{S1}] - \Delta\bar{V}_1^\circ(dP/dT)^\circ_{QAJ} + R \ln N_1} \tag{25}$$

Temperature-composition phase relations. From the data of Birch and LeComte (1960), Bell (1964), and Robie and Waldbaum (1968) we obtain $P_0 = -920$ bars; $(dP/dT)^\circ_{QAJ} = 20.684$ bar deg^{-1}; $\Delta\bar{V}_1^\circ = 0.40706$ cal bar^{-1} mole^{-1} (at 298°K and 1 atm) for the *quartz-albite-jadeite* equilibrium in the system SiO_2-$NaAlO_2$. Using these data with (25) and the Margules parameters in (1) we may calculate tentative feldspar compositions for the *quartz-alkali feldspar-jadeite* equilibrium at any pressure sure and temperature where quartz and jadeite are more stable than pure Na-feldspar. Isobaric temperature-composition diagrams are shown in Figure 10 for 16, 20, 26.11, and 32 kbar. The isothermal, isobaric composition diagrams in Figure 9 show (quantitatively) the calculated ternary relations in the silica-rich part of the system SiO_2-$KAlO_2$-$NaAlO_2$ for four temperatures at 20 kbar.

Seki and Kennedy (1964) studied the behavior of an orthoclase (approximately 73 mole percent $KAlSi_3O_8$) in a piston-cylinder apparatus in the range 700 to 1000°C and 20 to 40 kbar. The orthoclase was converted to a mixture of jadeite, quartz, and a more K-rich feldspar (92 ± 3 mole%) at 25 kbar and 730°C. The product feldspar formed in another experiment on the same starting material at 24 kbar and 600°C had a composition of 95 ± 3 mole percent $KAlSi_3O_8$. Equations (1) and (25) give 94.9 mole percent at 25 kbar and 730°C, and 98.4 mole percent at 24 kbar and 600°C, which are in reasonable agreement with the data of Seki and Kennedy (bearing in mind that our calculations have tacitly assumed that the alkali feldspars in this range are highly disordered sanidines,
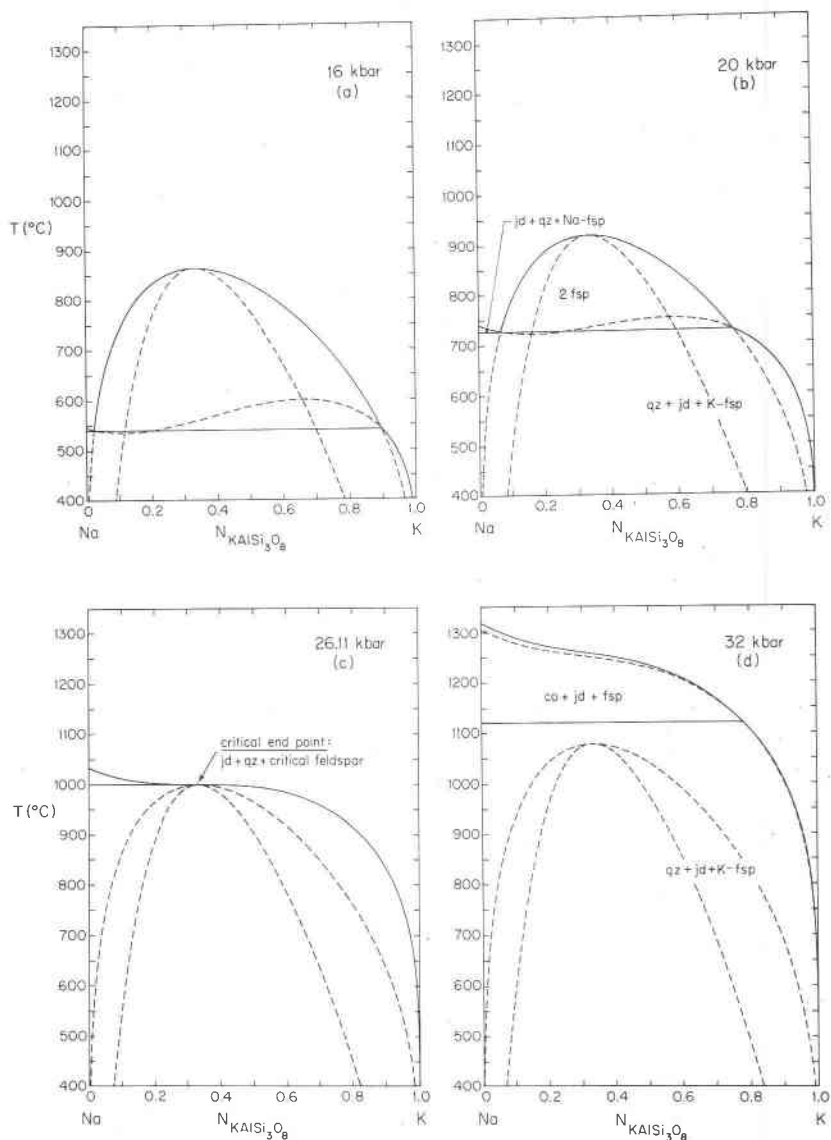
Fig. 10. Isobaric temperature-composition phase relations along the join NaAlSi$_9$O^8-KAlSi$_3$O$_8$ in the system NaAlO$_2$-KAlO$_2$-SiO$_2$ at 16, 20, 26.11, and 32 kbar. Dashed lines represent metastable or unstable phase boundaries and spinodal curves. Equilibrium relations with coesite are shown only at 32 kbar, and melting relations have been omitted (see Fig. 11).

which may not be so). A more detailed experimental investigation would be desirable, and would provide direct data on the quantity $(\mu_{1F}-\mu_{1F}°)$ which is needed to obtain more accurate estimates of the mixing properties of the feldspars involved.

The compositions of coexisting feldspars are also shown in Figures 9 and 10. The four-phase equilibrium representing the intersection of the alkali feldspar binodal surface with the P-T-N_{2F} surface for alkali feldspar coexisting with quartz and jadeite, can be calculated by simultaneous solution of (17) and the additional equilibrium conditions (6), or determined graphically by interpolation (the simplest method). This four-phase equilibrium is a univariant line in a P-T projection. It occurs at somewhat higher pressures and lower temperatures than the three-phase equilibrium for the K-free system as shown in Figure 11, and becomes practically indistinguishable from the 3-phase equilibrium for the K-free system at lower pressure and temperature.

At 999.5°C and 26.11 kbar the calculated four-phase equilibrium intersects the line of critical solution and terminates there at a critical endpoint at which the phases present are quartz, a critical feldspar, and jadeite. At higher pressures the line of critical solution is metastable (Figures 10 and 11). The critical end-point may be obtained directly from (3a), (3b), and (25).

Mineral facies. The system SiO_2-Al_2O_3-$NaAlO_2$-$KAlO_2$-H_2O is a useful one for considering many of the variations in mineral facies observed in pelitic schists (Thompson, 1961). The equilibria discussed above, combined with recent experimental results on the polymorphism of the aluminum silicates, on the phases of silica, and on melting relations in the sub-system SiO_2-$NaAlO_2$-$KAlO_2$ enable us now to construct a preliminary P-T diagram for the equilibria among the anhydrous phases in the silica-rich portion of this model system.

Key equilibria affecting quartz-bearing phase assemblages in the system SiO_2-Al_2O_3-$NaAlO_2$-$KAlO_2$ are shown in Figure 12. For the hydrous system these are the equilibria that are observed in the limit where the activity of H_2O in the fluid phase approaches zero. The diagrams in Figure 12 show schematically the compositions of phases coexisting with quartz, as projected through SiO_2 onto the plane Al_2O_3-$NaAlSi_3O_8$-$KAlSi_3O_8$ for the various pressure-temperature fields. (Compare with Figures 7 and 8 of Thompson, 1961.)

It must be borne in mind, however, that the relations shown in Figure 12 are, in most real assemblages, complicated by the presence of other components in certain of the phases. The fields of stability of jadeitic pyroxenes containing components such as $NaFeSi_2O_6$, $CaMgSi_2O_6$, and

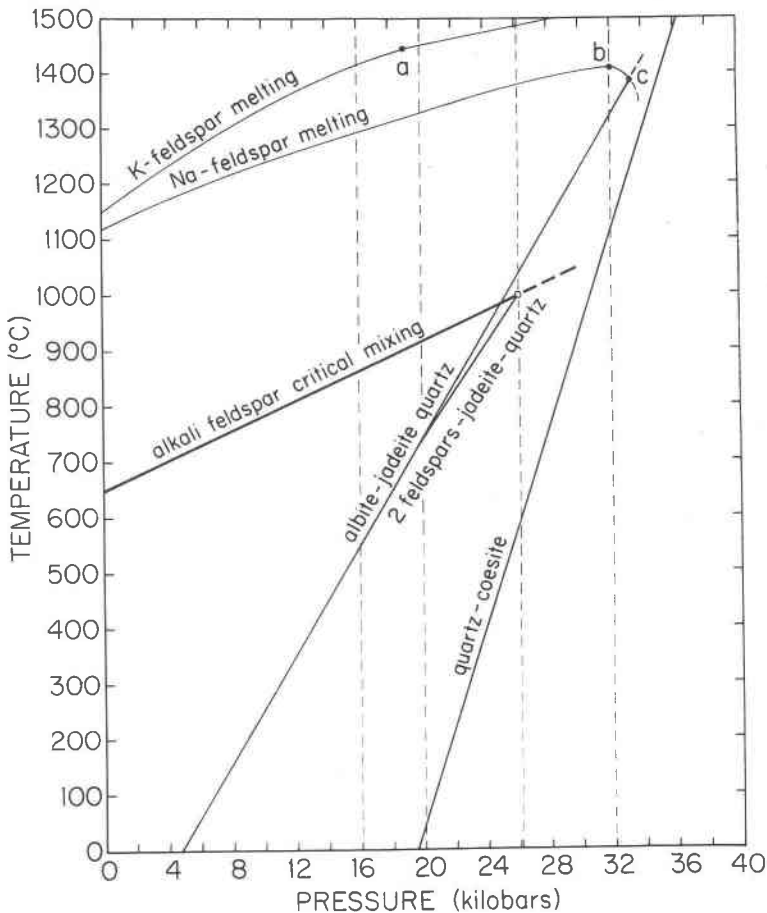Fɪɢ. 11. Tentative pressure-temperature diagram for some of the univariant equilibria in the silica-rich portion of the system SiO₂-NaAlO₂-KAlO₂. Quartz-coesite equilibrium after Boyd and England (1960); melting curve of albite (NaAlSi₃O₈) after Boyd and England (1963), Bell (1964); melting curve of pure sanidine (KAlSi₃O₈) after Lindsley (1966). Critical end-point (*quartz-jadeite-critical feldspar*) is shown as open circle. Dashed vertical lines correspond to the pressures of the $T-N$ diagrams in Figure 10. Invariant points a, b, and c involve liquid phases; see Bell (1964) and Lindsley (1966) for complete phase relations.

CaFeSi₂O₆, and coexisting with quartz and *alkali*-feldspar, will be somewhat more extensive than shown in Figure 12. The presence of the component CaAl₂Si₂O₈ in a feldspar, however, must force the pertinent equilibria the other way unless counterbalanced by a comparable content of CaAl₂SiO₆ in the jadeitic pyroxene, in which case the net effect is un-
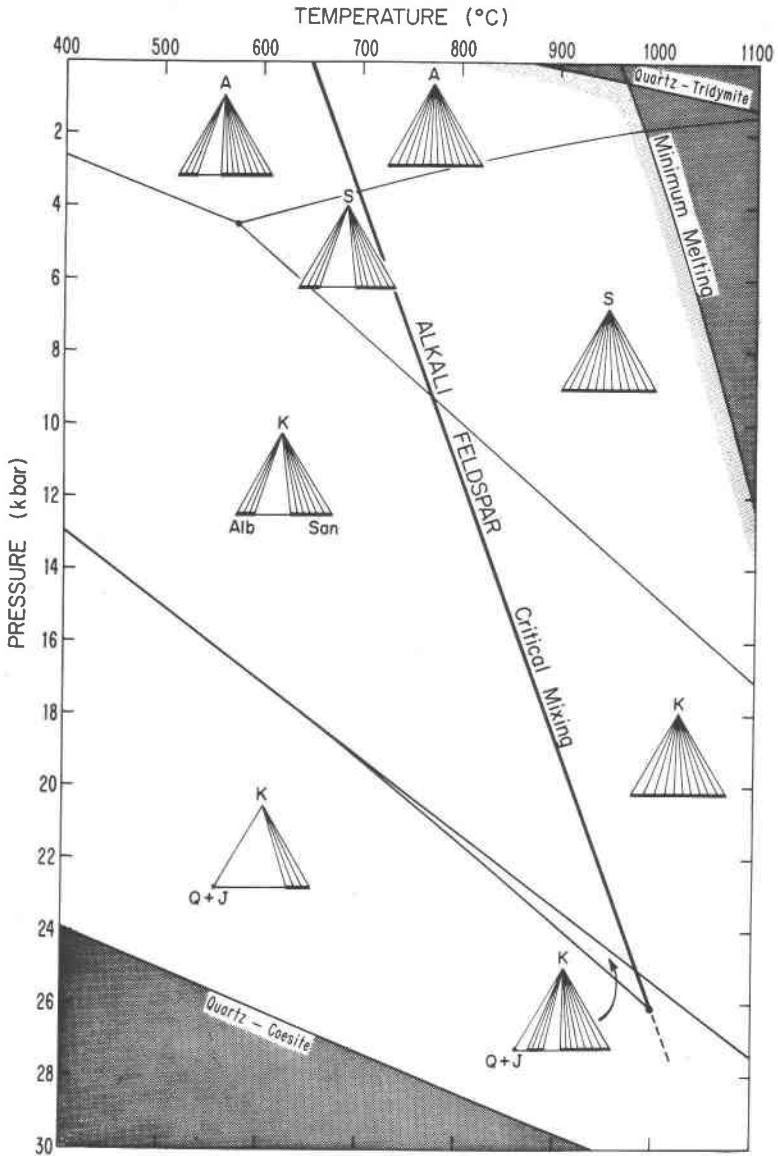
FIG. 12. Stability relations among jadeite, alkali feldspar, quartz, coesite, andalusite (A), kyanite (K), and sillimanite (S). The *andalusite-kyanite-sillimanite* invariant point is shown here as at $575 \pm 15°C$ and 4.5 ± 0.3 kbar based on the data of Newton (1966), Holm and Kleppa (1966), and Richardson, Bell, and Gilbert (1968). *Quartz-tridymite* equilibrium curve and minimum melting temperature (960°C) in the silica-rich portion of the system SiO_2-$NaAlO_2$-$KAlO_2$ at 1 bar after Tuttle and Bowen (1958). Anhydrous minimum melting curve assumed to have approximately the same slope as melting curve of pure albite (Fig. 11). Schematic isothermal-isobaric sections refer only to quartz-bearing assemblages.

certain. It must also be emphasized that all of the equilibria, experimental or calculated, in Figure 12 are tentative and that they should be revised as new data appears. One important area in which further data are needed is on the effect of Al-Si ordering on the equations of state for alkali feldspars.

Note added in proof: In a more recent paper just received by us, Perchuk and Andrianova (1968, Thermodynamic equilibria of alkali feldspars $(K, Na)AlSi_3O_8$ with aqueous $(K, Na)Cl$ solutions from 500–700°C and 2000-1000 bars pressure. In *Experimental and Theoretical Investigations of Mineral Equilibria*, Izd-vo "Nauka," Moscow, p. 37–72) consider explicitly the effect of excess volume on the mixing properties of sanidine.

REFERENCES

BACHINSKI, S. W., AND P. M. ORVILLE (1968) Experimental determination of the microcline—low albite solvus and interpretation of the crystallization histories of perthites (abstr.). *Geol. Soc. Amer. Ann. Meet., Mexico City, Prog.* p. 15.

BELL, P. M. (1964) High pressure melting relations for jadeite composition. *Carnegie Inst. Wash. Year Book* **63**, 171–174.

BIRCH, F., AND P. LECOMTE (1960) Temperature-pressure plane for albite composition. *Amer. J. Sci.* **258**, 209–217.

BOETTCHER, A. L., AND P. J. WYLLIE (1968) Jadeite stability measured in the presence of silicate liquids in the system $NaAlSiO_4$-SiO_2-H_2O. *Geochim. Cosmochim. Acta* **32**, 999–1012.

BOYD, F. R., AND J. L. ENGLAND (1960) The quartz-coesite transition. *J. Geophys. Res.* **65**, 749–756.

———, AND ——— (1963) Effect of pressure on the melting of diopside, $CaMgSi_2O_6$, and albite, $NaAlSi_3O_8$, in the range up to 30 kilobars. *J. Geophys. Res.* **68**, 311–323.

GOLDSMITH, J. R., AND F. LAVES (1961) The sodium content of microclines and the microcline-albite series. *Cursillos Conf. Inst. Lucas Mallada* **8**, 81–96.

HALA, E., J. PICK, V. FRIED, AND O. VILIM (1967) *Vapour-Liquid Equilibrium.* Pergamon Press, Oxford, 599 p.

HLABSE, T., AND O. J. KLEPPA (1968) The thermochemistry of jadeite. *Amer. Mineral.* **53**, 1281–1292.

HOLM, J. L., AND O. J. KLEPPA (1966) The thermodynamic properties of the aluminum silicates. *Amer. Mineral.* **51**, 1608–1622.

KRACEK, F. C., K. J. NEUVONEN, AND G. BURLEY (1951) Thermochemistry of mineral substances. I. A thermodynamic study of the stability of jadeite. *J. Wash. Acad. Sci.* **41**, 373–383.

LINDSLEY, D. H. (1966) Melting relations of KAlSi$_3$O$_8$: effect of pressure up to 40 kilobars. *Amer. Mineral.* **51**, 1793–1798.

MUELLER, R. F. (1964) Theory of immiscibility in mineral systems. *Mineral. Mag.* **33**, 1015–1023.

NEWTON, M. S., AND G. C. KENNEDY (1968) Jadeite, analcite, nepheline, and albite at high temperatures and pressures. *Amer. J. Sci.* **266**, 728–735.

NEWTON, R. C. (1966) Kyanite-andalusite equilibrium from 700° to 800°C. *Science* **153**, 170–172.

PERCHUK, L. L., AND I. D. RYABCHIKOV (1968) Mineral equilibria in the system nepheline —alkali feldspar—plagioclase and their petrological significance. *J. Petrology* **9**, 123–167.

RICHARDSON, S. W., P. M. BELL, AND M. C. GILBERT (1968) Kyanite-sillimanite equilibrium between 700° and 1500°C. *Amer. J. Sci.* **266**, 513–541.

ROBERTSON, E. C., F. BIRCH, AND G. J. F. MACDONALD (1957) Experimental determination of jadeite stability relations to 25,000 bars. *Amer. J. Sci.* **255**, 115–137.

ROBIE, R. A., AND D. R. WALDBAUM (1968) Thermodynamic properties of minerals and related substances. *U. S. Geol. Surv. Bull.* **1259**, 256 pp.

SCATCHARD, G. (1940) The calculation of the compositions of phases in equilibrium. *J. Amer. Chem. Soc.* **62**, 2426–2429.

SCHAIRER, J. F. (1950) The alkali feldspar join in the system NaAlSiO$_4$-KAlSiO$_4$-SiO$_2$. *J. Geol.* **58**, 512–517.

SEKI, Y., AND G. C. KENNEDY (1964) The breakdown of potassium feldspar, KAlSi$_3$O$_8$, at high temperatures and high pressures. *Amer. Mineral.* **49**, 1688–1706.

SELTZ, H. (1935) Thermodynamics of solid solutions. II. Deviations from Raoult's Law. *J. Amer. Chem. Soc.* **57**, 391–395.

THOMPSON, J. B., Jr. (1961) Mineral facies in pelitic schists. *In* G. A. Sokolov, (ed.,) *Physico-chemical Problems in the Formation of Rocks and Mineral Deposits,* D. S. Korzhinsky commemorative vol. Akad Nauk SSSR, Moscow, p. 313–325 [in Russian with English summary].

——— (1967) Thermodynamic properties of simple solutions. in P. H. Abelson, (ed.,) *Researches in Geochemistry II,* John Wiley and Sons, New York, p. 340–361.

———, (1969) Chemical reactions in crystals. *Amer. Mineral. 54,* 341–375.

——— AND D. R. WALDBAUM (1967) Thermodynamic mixing properties of sanidine/high-albite crystalline solutions (abstr.). *Trans. Amer. Geophys. Union* **48**, 230.

———, AND ——— (1968) Mixing properties of sanidine crystalline solutions. I. Calculations based on ion-exchange data. *Amer. Mineral.* **53**, 1965–1999.

———, AND ——— (1969) Mixing properties of sanidine crystalline solutions. III. Calculations based on two-phase data. *Amer. Mineral.* **54**, 811–838.

TUTTLE, O. F., AND N. L. BOWEN (1958) Origin of granite in light of experimental studies in the system NaAlSi$_3$O$_8$-KAlSi$_3$O$_8$-SiO$_2$-H$_2$O. *Geol. Soc. Amer. Mem.* **74**, 153 pp.

WALDBAUM, D. R. (1966) *Calorimetric Investigation of the Alkali Feldspars.* Ph.D. Thesis, Harvard University, 247 pp.

——— (1968) High-temperature thermodynamic properties of alkali feldspars. *Contrib. Mineral. Petrology* **17**, 71–77.

——— (1969) Crystal-liquid phase relations in the system Na(AlSi$_3$O$_8$)−K(AlSi$_3$O$_8$). (abstr.) *Trans. Amer. Geophys. Union* **50**, 351.

———, AND J. B. THOMPSON, JR. (1968) Mixing properties of sanidine crystalline solutions. II. Calculations based on volume data. *Amer. Mineral.* **53**, 2000–2017.